IEEE Access
Multidisciplinary | Rapid Review | Open Access Journal

SPECIAL SECTION ON HUMAN-DRIVEN EDGE COMPUTING (HEC)

Received March 13, 2020, accepted March 23, 2020, date of publication March 25, 2020, date of current version April 22, 2020.

Digital Object Identifier 10.1109/ACCESS.2020.2983252

Hybrid Entangled States With Multi-Degree of Freedom and High Purity for Internet of Vehicles

JIANJUN GUO[1], KEQIANG WANG[1], FENGMEI YU[1,2], AND KEN CAI[1]

[1]College of Automation, Zhongkai University of Agriculture and Engineering, Guangzhou 510225, China
[2]School of Engineering and the Built Environment, Edinburgh Napier University, Edinburgh EH10 5DT, U.K.

Corresponding author: Ken Cai (icken@zhku.edu.cn)

This work was supported in part by the Innovation and Entrepreneurship Program for Undergraduate Universities in Guangdong Province under Grant 2018A022758, in part by the Educational Cooperation and Education Project of the Ministry of Education under Grant 201802048037, Grant 201802299045, and Grant 201901096025, in part by the Special Funding Project for Excellent Doctoral Talents under Grant KA180530512, in part by the Guangzhou Science and Technology Program under Grant 201704050001, in part by the Natural Science Foundation of Guangdong Province under Grant 2016A030310234, and in part by the Guangdong Provincial Science and Technology Program under Grant 2017A040405056.

ABSTRACT The development of intelligent Internet of vehicles (IoV) is based on communication technology, especially the quantum communication of hybrid entangled states based on orbital angular momentum (OAM). The quantum key distribution (QKD) method is demonstrated using hybrid entangled states with multi-degree of freedom and high purity based on OAM. First, the polarization entangled photon pairs are produced by two type I BBO crystals by means of spontaneous parametric down-conversion (SPDC). The polarization-OAM hybrid entangled states are created by q-plate (QP) to realize QKD. It is found that the polarization entangled photon pairs have the characteristics of OAM. A single mode fiber (SMF) is proposed to filter the topological charge non-zero photons and purify the polarization entangled photon pairs. Then the purification setup with M-Z interferometer and beam rotator (BR) is presented which can purify the polarization-OAM hybrid entangled states. The high purity polarization-OAM hybrid entangled states are implemented, and the QP conversion rate of 3 secondary feedbacks is 99.84% theoretically. Analysis indicates that precise purity polarization-OAM hybrid entangled state can increase the fidelity of information and improve the anti-interference ability in this program without mutually unbiased bases (MUBs). The photon utilization rate, energy-efficient and low-latency communication can be greatly improved by using the OAM carrying information.

INDEX TERMS Internet of vehicles (IoV), low-latency, orbital angular momentum (OAM), high purity, hybrid entanglement, coincidence measurement.

I. INTRODUCTION

The Internet of vehicles (IoV) is an important intersection of the Internet of things (IoT) and intelligent vehicles in strategic emerging industries [1], [2]. Intelligent IoT is a kind of IoT that can collect, identify, transmit, integrate and utilize vehicle information, and can realize intelligent identification, positioning, tracking, monitoring and management. It is considered to be the most easy application of IoT to form system standards and have the most industrial potential [3]–[7]. The Intelligent IoV architecture is reported in Figure 1. The development of intelligent IoV is based on communication technology, especially the quantum communication of hybrid entangled states based on orbital angular momentum (OAM). Quantum entanglement [8], [9] is the relation, which is non-localized and non-classical between two or more particles subsystems.

Quantum entanglement possesses unique characteristics within the maximum entangled state of all degrees of freedom, and perform quantum dense coding [10], ghost imaging [11], quantum teleportation [12], [13], energy-efficient and low-latency communication and computation, and other important applications [14], [15]. Quantum information processing based on entanglement photon pairs can achieve

The associate editor coordinating the review of this manuscript and approving it for publication was Rongbo Zhu.

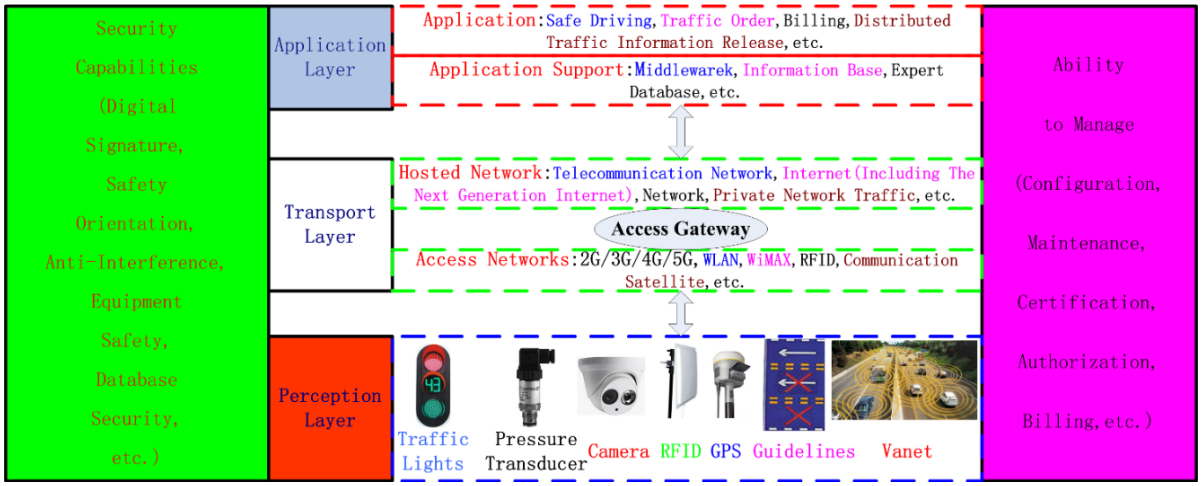

FIGURE 1. Intelligent Internet of vehicles architecture.

quantum key distribution (QKD), which has outstanding features of large capacity and strong confidentiality. Since the E91 protocol [16] is put forward, QKD based on entangled photon pairs has attracted great attention [17]–[23]. In 1988, Ou and Mandel [24], from University of Rochester, were the first individuals to obtain the polarization entangled states of two-photon, which could implement QKD [18]–[20] with coding information of double qubits, by spontaneous parametric down-conversion (SPDC). This provides the probability of hybrid entanglement in combination with other degrees of freedom; OAM is a different degree of freedom and carries considerable encoding information. In 1992, Allen team [25] in Leiden University proposed that photons contain certain OAM $l\hbar$. Encoding information using photon OAM increases the information transmission capacity [26], [27]. The eigenstate of the OAM is an infinite dimensional state. If we use the high-dimensional feature of OAM to encode information, then we can fulfill the QKD, which has many qubits and high security [21]–[23]. This provides theoretical basis for quantum communication of the single photon with mutli-qubit. In 2001 Mair team [28] was the first to report the realization of entanglement using the OAM of photons by adopting SPDC. The entangled states of two-photon OAM can be experimentally used for QKD protocol [21], [22]. However, the programs can only be encoded and modulated at low dimension because they are entangled states of single degree of freedom photon pairs.

Hybrid entangled states [29], [30] demonstrate entanglement between different degrees of freedom of multiple-photon. The hybrid entangled between OAM, polarization and various degrees of freedom can make asymmetric QKD exist. In 2010 Eleonora Nagali and Fabio Sciarrino [31] reported the first success of hybrid polarization-OAM entangled states by adopting a SPDC source of polarization entangled states and a polarization-OAM transferrer.

The QKD using the polarization-OAM hybrid entangled states opens the possibility to exploit the features of the higher-dimensional space of OAM state to encode information, but there are still several problems to be improved. First, density matrix of the hybrid entangled states is not reconstructed. Second, the polarization-OAM hybrid entangled states are not pure and the utilization rate is not high. Third, in order to make the QKD scheme go smoothly, the purification rate analysis, security analysis and high-dimensional encoding of multi-degree of freedom should be carried out.

A purification device is proposed in this paper to solve the problems above. The contributions of this paper are summarized as follows.

1) Density matrix of the hybrid entangled states is reconstructed by adopting quantum state tomography technology.
2) A purification device, which is used for producing high purity polarization-OAM hybrid entangled states, is proposed. And the purification rate is analyzed.
3) A QKD project, which adopts the modulation of precise-purity polarization-OAM hybrid entangled states, uses OAM to encode information, introduces coincidence measurement, and achieves quantum communication with a large capacity and high efficient. In this paper, the mutually unbiased bases (MUBs) are not employed, which lead to a simpler scheme without the need of a classical channel. The QKD project is not notably susceptible to the effects of experimental conditions and the environment noise. And it has high fidelity of information. The photon utilization rate can be improved with the amount of information for $Log_2^m + 1$ by using the OAM carrying information.

This paper organized as follows. Section II introduce polarization-OAM hybrid entangled states, purification of hybrid entangled states. The QKD system design presented in Section III. Section IV proposes the performance analysis. The purification rate analysis, security analysis and high-dimensional encoding of multi-degree of freedom are conducted in Section IV, and Section V concludes this paper.

II. QKD BASED ON POLARIZATION-OAM HYBRID ENTANGLEMENT

A. GENERATION OF POLARIZATION-OAM HYBRID ENTANGLED STATES

Polarization-OAM entanglement is a hybrid entanglement between different degrees of freedom of multi-photon. The two photons system with these hybrid entangled states violates Bell's inequalities. The entanglement properties of these hybrid entangled states are used to implement asymmetric QKD. The polarization-OAM hybrid entangled state [22] is expressed as:

$$|\Phi\rangle_{hybrid} = \frac{1}{\sqrt{2}}(|L\rangle_A^{\pi}|-1\rangle_B^0 + |R\rangle_A^{\pi}|+1\rangle_B^0) \tag{1}$$

where $|.\rangle^0$ denotes the right vector of OAM, $|L\rangle$ and $|R\rangle$ denote the left and right circular polarization states, respectively. Subscripts A and B denote the signal and idle photons, respectively. To completely characterize the hybrid entangled states in Equation (1), we reconstructed the density matrix of the quantum states by adopting quantum state tomography technology [32], [33]. In the field of quantum information, the fidelity is used to measure similarity between two states, however, it's not a metric of density matrix in the space. The hybrid entangled state can be abbreviated to $|\Phi\rangle = \frac{1}{\sqrt{2}}(|L\rangle|-1\rangle + |R\rangle|+1\rangle)$, with the two relations: $|L\rangle = \frac{1}{\sqrt{2}}(|H\rangle - i|V\rangle)$ and $|R\rangle = \frac{1}{\sqrt{2}}(|H\rangle + i|V\rangle)$. Bringing $|L\rangle = \frac{1}{\sqrt{2}}(|H\rangle - i|V\rangle)$ and $|R\rangle = \frac{1}{\sqrt{2}}(|H\rangle + i|V\rangle)$ to $|\Phi\rangle = \frac{1}{\sqrt{2}}(|L\rangle|-1\rangle + |R\rangle|+1\rangle)$, we can get

$$\begin{aligned}|\Phi\rangle &= \frac{1}{\sqrt{2}}(|L\rangle|-1\rangle + |R\rangle|+1\rangle)\\ &= \frac{1}{2}[|H\rangle|-1\rangle + |H\rangle|+1\rangle - i|V\rangle|-1\rangle + i|V\rangle|+1\rangle]\end{aligned}$$

Then the density matrix of hybrid entangled state is

$$\vec{\rho} = |\Phi\rangle\langle\Phi| = \frac{1}{2}\begin{bmatrix}2 & 1+i\\ 0 & 1-i\end{bmatrix} \otimes \frac{1}{2}\begin{bmatrix}2 & 0\\ 1-i & 1+i\end{bmatrix} = \begin{bmatrix}1 & 0 & \frac{1}{2}+\frac{1}{2}i & 0\\ \frac{1}{2}-\frac{1}{2}i & \frac{1}{2}+\frac{1}{2}i & \frac{1}{2} & \frac{1}{2}i\\ 0 & 0 & \frac{1}{2}-\frac{1}{2}i & 0\\ 0 & 0 & -\frac{1}{2}i & \frac{1}{2}\end{bmatrix}$$

The real part of the density matrix is

$$\begin{bmatrix}1 & 0 & \frac{1}{2} & 0\\ \frac{1}{2} & \frac{1}{2} & \frac{1}{2} & 0\\ 0 & 0 & \frac{1}{2} & 0\\ 0 & 0 & 0 & \frac{1}{2}\end{bmatrix},$$

and the imaginary part of the density matrix is

$$\begin{bmatrix}0 & 0 & \frac{1}{2}i & 0\\ -\frac{1}{2}i & \frac{1}{2}i & 0 & \frac{1}{2}i\\ 0 & 0 & -\frac{1}{2}i & 0\\ 0 & 0 & -\frac{1}{2}i & 0\end{bmatrix}.$$

Thus, the experimental results of the density matrix $\rho_{\pi,0}^{A,B}$ are depicted in Figure 2, with the elements of the density matrix expressed in the polarization and OAM basis $\{|L,+1\rangle, |L,-1\rangle, |R,+1\rangle, |R,-1\rangle\}$. Quantum state tomography technology, which is a type of statistical measurement, can effectively achieve the quantum state measurement, and obtain all the state information. It follows that the polarization-OAM hybrid entangled states have the advantages of easy calibration, high quality, and a bright generation rate.

The conversion rate of QP is commonly 0.80 ± 0.05 in the process of translating polarization into OAM, at the same time a deviation value that polarization entangled states have not been transformed is 0.20 ± 0.05 [24]. In particular, the polarization entangled states under the effect of QP are still in our plan. If we use the polarization-OAM hybrid entangled states whose purity is not high in communication system, it will lead to communication system the information distortion, and be easily influenced by experimental condition and environmental noise. In order to acquire precise purity polarization-OAM hybrid entangled states, the following will design a solution.

B. PURIFICATION OF HYBRID ENTANGLED STATES

The characteristics of polarization-OAM hybrid entangled states are described as Equation (1). It turned out that the transformation from the polarization state to the OAM state is incomplete, which is caused by the characteristics of devices such as QP. That is, polarization entangled states remain in the preparation of polarization–OAM hybrid entangled states [31]. It is necessary to perform accurately within the purity polarization-OAM hybrid entangled states, in order to maintain high fidelity within the QKD. A M-Z interferometer and a beam rotator (BR) [34], [35] are used to design a purification project, which is depicted as Figure 3. In practical application, a BR is inserted into one arm of the M-Z interferometer, whose rotation angle is 2α. When the beam coming out from QP goes through the BR, the beam carrying phase $\exp(il\phi)$ will produce phase difference $\delta = 2l\alpha$ between two arms of M-Z interferometer. However, when the beam carrying not phase $\exp(il\phi)$ but polarization goes through the BR, there is not phase difference.

When the input state $(|in\rangle_{BS_{A1}} = |0\rangle|1\rangle)$, where $|0\rangle$ and $|1\rangle$ correspond to the vacuum and single-photon states, goes into the purification setup through the beam splitter (BS_{A1}) after the purification effect of the purification setup, the output

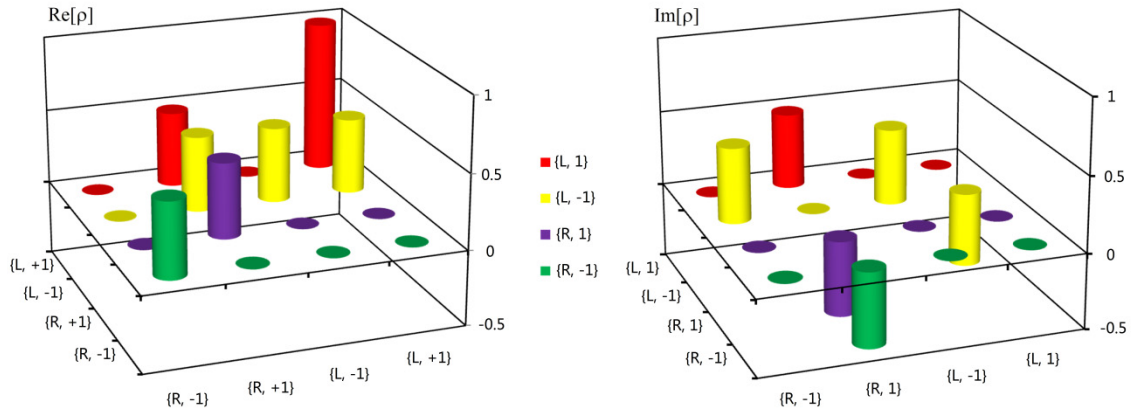

FIGURE 2. Density matrix of the hybrid entangled states.

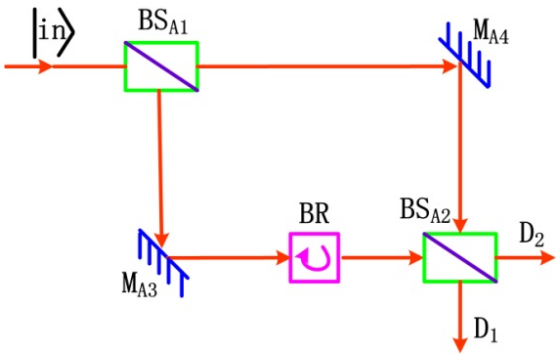

FIGURE 3. Purification setup. BS_{A1}, BS_{A2}: beam splitter; M_{A3}, M_{A4}: mirrors with high reflectance film; BR: beam rotator.

state of BS_{A2} is described as

$$|out\rangle_{BS_{A2}} = \frac{1}{2}(1 - e^{i\delta})\,|0\rangle\,|1\rangle + \frac{i}{2}(1 + e^{i\delta})\,|1\rangle\,|0\rangle \qquad (2)$$

When $\alpha = \pi/2$, that is, $\delta = \pi$, the photon carrying the state $|1\rangle$ will generate destructive interference in the $BS_{A2,}$ and come out from the export detector (D_2) of the purification setup. By contrast, the photon carrying state $|0\rangle$ will generate a constructive interference in the BS_{A2} and come out from the export (D_1) of the purification setup.

In practice, the quantum state $|\varphi_2\rangle_{l=0}^{\pi} + |\varphi_2\rangle_{l\neq 0}^{0}$ is sent into the purification setup, after purification effect, the photon carrying hybrid entangled state $|\Phi\rangle_{hybrid}$ as Equation (1) with the OAM of $|l = 1\rangle$ and $|l = -1\rangle$ will attract destructive interference in the $BS_{A2,}$ and come out from the export D_2 of the purification setup. Additionally, after the purification of specific optical structure and the filtration of single mode fiber (SMF) in the link, the very weak photons carrying not hybrid entangled state which is residuary can be seen as the OAM state whose topological charge is zero, that is, $|l = 0\rangle$. Moreover, these photons can generate constructive interference in the BS_{A2} and come out from the export (D_1) of the purification setup. The output state $|\varphi_2\rangle_{l=0}^{\pi}$, which will be ignored and dismissed, can be described as $\frac{1}{\sqrt{2}}(|L\rangle'_A\,|R\rangle'_B + |R\rangle'_A\,|L\rangle'_B)$. For this reason, the preparation of high purity hybrid entangled states can come out from the export D_2.

The experiment results show that polarization-OAM hybrid entangled states are desirable for quantum information and communication protocols, such as quantum teleportation [36], and for the possibility to send quantum information through an optical quantum network composed of optical fiber channels and free-space. When precise purity polarization-OAM hybrid entangled states merge with quantum coding information, they can carry out QKD. This results in low requirements on the experimental conditions and the surrounding environment, and with high fidelity. These provide a theoretical basis for QKD, although the QKD scheme has not seen applicable as of yet.

The proposed principle block diagram of the solution is exhibited in Figure 4. High-purity polarization-OAM hybrid entangled states are used, goes to modulate the polarization state of the signal photon and the N-dimension OAM state of the idle photon carrying quantum information, have on QKD, and achieve quantum communication, which is high-dimensional modulation and high-efficiency.

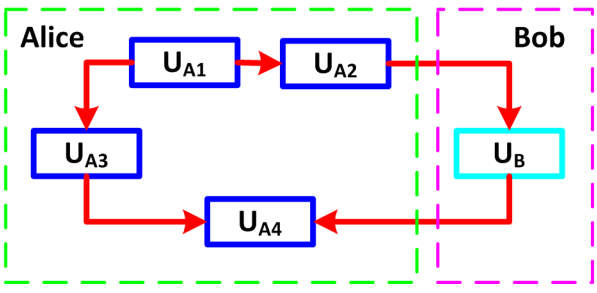

FIGURE 4. Principle block diagram of QKD based hybrid entangled states. U_{A1}: hybrid entangled states generation unit; U_{A2}: hybrid entangled states purification unit; U_{A3}: polarization modulation unit; U_{A4}: coincidence measurement and decoding unit; U_B: OAM modulation unit.

III. QKD SYSTEM DESIGN

The QKD system diagram based on polarization-OAM hybrid entangled states of two photons is depicted in Figure 5. There are composed of hybrid entangled states generation unit U_{A1}, hybrid entangled states purification unit U_{A2}, polarization modulation unit U_{A3}, and coincidence measurement and decoding unit U_{A4} in Alice's private space. Where hybrid entangled states generation unit U_{A1}; this component contains a quasi-continuous-wave mode-locked (100 MHz) 355 nm laser diode (LD), two BBO crystals cut for Type-I phase matching, SMF_{A1}, a polarization controller (PC), and a QP [37]. The hybrid entangled state purification unit U_{A2} is mainly used for purifying polarization–OAM hybrid entangled states; this unit contains BS_{A1}, BS_{A2}, two dove prisms (DP_{A1} and DP_{A2}) and four mirrors (M) with high-reflective film (M_{A2}, M_{A3}, M_{A4} and M_{A5}), is mainly used for purifying polarization-OAM hybrid entangled states. Polarization modulation unit U_{A3}, which contains M_{A1}, quarter wave plate (QWP), half wave plate (HWP), polarization beam splitter (PBS) and f = 1.6mm lens, is mainly used for modulating polarization by means of phase deviation. Coincidence measurement and decoding unit U_{A4}, which contains two D (D_{A1} and D_{A2}) and Coincidence Counter (TCSPC), is mainly used for detecting the coming photons from SMF, sending detection results to coincidence measurement and decoding. There is composed of OAM modulation unit U_B in Bob's private space. This OAM modulation unit U_B which contains spatial light modulator (SLM) controlled by the computer and f = 1.6mm lens, is mainly used for modulating OAM by means of the designed phase hologram.

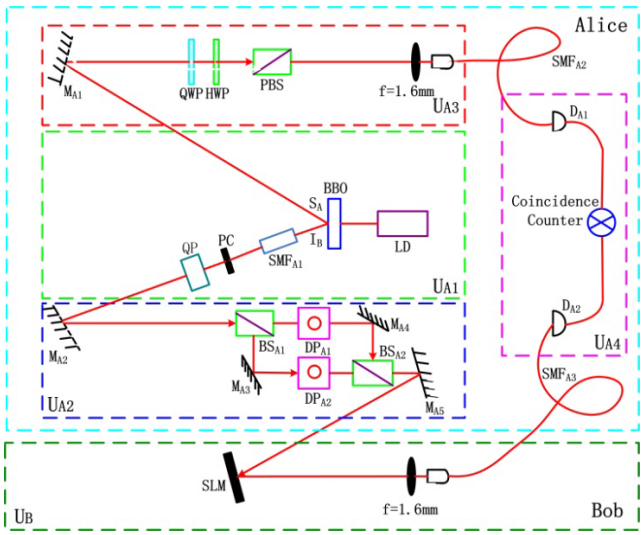

FIGURE 5. QKD system schematic diagram of polarization-OAM hybrid entangled states.

In practice, two BBO crystals [38] cut for type-I phase matching by means of the vertical pump which is produced by the LD generate by adopting SPDC polarization entangled pairs, that is, the signal photon and the idle photon. As shown in Figure 5, S_A road for the signal photons A, I_B road for the idle photons B, and the quantum states $|\psi_1\rangle$ that comes out of the BBO crystals are expressed in $|\varphi_1\rangle_{l=0}^{\pi} + |\varphi_1\rangle_{l\neq 0}^{0}$.

In order to eliminate the potential OAM entanglement [31], the idle photons in the I_B light path are coupled into the SMF, which collapses the transverse spatial mode into a pure TEM00, corresponding to OAM state with m = 0. Thereby, the possible OAM entanglement can be cancelled out. The polarization entangled pairs, corresponding to OAM state with m = 0, are prepared, whose quantum state $|\psi_2\rangle_{l=0}^{\pi}$ is depicted as $\frac{1}{\sqrt{2}}(|H\rangle_A|H\rangle_B + |V\rangle_A|V\rangle_B)$.

Here, the polarization entangled pairs carrying OAM state with m = 0 through the PC can compensate the polarization rotation introduced by the SMF that enters the QP. The QP then transforms the polarization quantum states into the OAM degree of freedom.

Due to the constraints of the QP device material performance, in theory there are less than 80% idle photons B, which are transformed into polarization-OAM hybrid entangled photons, and whose quantum states $|\Phi\rangle_{hybrid}$ are expressed as Equation (1).

As stated above, in the S_A light path, due to the entanglement of the quantum states $|\Phi\rangle_{hybrid}$ are shown in Equation (1).

As a matter of fact, there are more than 20% residual polarization entangled photons that are not transformed. Thus, the signal photons A and the idle photons B are not precise-purity polarization-OAM hybrid entangled photons. If these hybrid entangled photons are used to encode quantum information for quantum communication and quantum computation, quantum coding information will lead to information distortion, and be susceptible to experimental condition and environmental noise.

The measurement of the polarization degree of freedom does not affect the OAM. Thus, to reduce the system error rate and outside influence, we will send polarization entangled photons, which are not transformed, and polarization-OAM hybrid entangled photons to the system, which is used for purification, as displayed in Figure 3. The quantum states of the polarization entangled photons, which are not transformed, are presented in $\frac{1}{\sqrt{2}}(|L\rangle'_A|R\rangle'_B + |R\rangle'_A|L\rangle'_B)$. If these quantum states are filtered out, the photons of high purity polarization-OAM hybrid entangled states can be acquired.

In the practical transmission path, the idle photons coming out from the QP through the BS_{A1} enter the purification setup. When the input is $|\psi_3\rangle = |\varphi_2\rangle_{l\neq 0}^{0} + |\varphi_2\rangle_{l=0}^{\pi}$, the output of the BS_{A2} through the effect of the purification setup is:

$$|out\rangle'_{BS_{A2}} = \frac{1}{2}(1-e^{i\delta})\,|\varphi_2\rangle_{l=0}^{\pi}\,|\varphi_2\rangle_{l\neq 0}^{0} + \frac{i}{2}(1+e^{i\delta})|\varphi_2\rangle_{l\neq 0}^{0}\,|\varphi_2\rangle_{l=0}^{\pi} \quad (3)$$

When $\alpha = \pi/2$, that is, $\delta = \pi$, $l = 1$, thus, the photons carrying the quantum state expressed as Equation (1) occur destructive interference in the BS_{A2}, and will come out from the BS_{A2} of the purification setup.

High purity polarization-OAM hybrid entangled states are obtained after the above-mentioned transmission path, and are adopted for modulating and encoding. There is an angle of 45° between the incident vibration plane of polarized light and the Optical axis of QWP, which is the point where the polarized light goes through the QWP, and is transformed into the circular polarized light. If there is an angle of $\theta/2$ between the fast axis of HWP and x axis, the Jones matrix of the HWP is $G = \begin{bmatrix} \cos\theta & \sin\theta \\ \sin\theta & -\cos\theta \end{bmatrix}$. When the circular polarized light passes through HWP, there is an angle of θ between the vibrating surface of its resultant vibration and the vibrating surface of the incident circular polarized light. Here, the HWP and the PBS are used together. If the HWP is revolved at this time, then we can acquire the desired variable rotation angle. In Alice's private space, the quantum states of high purity signal photons through the modulating action of the QWP, the HWP and the PBS are expressed as:

$$|\theta\rangle^{\pi} = \frac{1}{\sqrt{2}}(e^{i\theta}\,|L\rangle_A^{\pi} + e^{-i\theta}\,|R\rangle_A^{\pi}) \tag{4}$$

where $\theta/2$ is a variable rotation angle, which is related to the HWP and the horizontal direction. The polarization states are modulated by means of the random variable rotation angle θ and used to load information. The signal photons A come out from the PBS through the lens (f = 1.6mm), and are directly coupled into the SMF_{A2}, and then sent to the D_{A1}.

In Bob's private space, high purity idle photons B are used to modulate and encode by means of the SLM (Holoeye Pluto BB) controlled by the computer. The phase holograms of the idle photons are defined by the sector states changing with an arbitrary relative phase, which is on behalf of a point along the equator. The OAM states are modulated and loaded information by the sector states by means of the random variable rotation angle. In the diffraction, the holographic pattern can transform the superposition states $|\chi\rangle^0$ of the OAM into fundamental-mode Gaussian states TEM00. The superposition states $|\chi\rangle^0$ of OAM modulated by the SLM with the controlling of the computer are depicted as:

$$|\chi\rangle^0 = \frac{1}{\sqrt{2}}(e^{i\chi}\,|+1\rangle_B^0 + e^{-i\chi}\,|-1\rangle_B^{\pi}) \tag{5}$$

When compared with the linear polarization, the superposition states $|\chi\rangle^0$ of OAM are spatial mode, and the angle χ can be regarded as the 'direction angle' of the spatial mode. After the modulation of the SLM controlled by the computer, the idle photons B through the lens (f = 1.6mm) are coupled into the SMF_{A3}, and then sent to the D_{A2}.

When the high purity hybrid entangled Bell states of the signal photons A and the idle photons B are expressed as Equation (1), the D_{A1} and D_{A2}, respectively detect the photons coming out from the SMF_{A2} and SMF_{A3} at the same time, and send the detection results to the coincidence counter for coincidence measurement and decoding. We aim to use the following coincidence rate $P(\theta, \chi)$ to detect the Bell of A and B, and the coincidence rate $P(\theta, \chi)$ is depicted as:

$$P(\theta, \chi) = \left|\langle\Phi|_{hybrid} \cdot |\theta\rangle^{\pi}|\chi\rangle^0\right|^2 \propto \cos^2(\chi - \theta) \tag{6}$$

where θ denotes the random variable rotation angle of the polarization states, and χ denotes the random variable angle of the OAM sector states.

Based on the above analysis, the actual light path of the QKD process is as follows:

1) After laser pulse through the BBO crystals, Alice can produce polarization entangled photon pairs, including one for the signal photons, and another for the idle photons. In the idle photons transmission path, the polarization photons carrying the OAM with topological charge $l \neq 0$ are filtered by the SMF_{A1}. The QP can transform the polarization entangled photon carrying the OAM with a topological charge $l = 0$ into the polarization-OAM hybrid entangled photons. High purity polarization-OAM hybrid entangled photons are obtained, after the effect of purification setup.
2) In Alice's private space, according to the entanglement properties, the quantum states of the signal photons carrying high purity polarization-OAM hybrid entangled states are the quantum states $|\theta\rangle_A^{\pi}$, which are here used polarization to modulate changing with variable phase through the QWP, the HWP and the PBS.
3) Meanwhile, in Bob's private space, the quantum states of the idle photons are high purity sector states $|\chi\rangle_B^0$ of polarization-OAM hybrid entanglement that are produced by the SLM with the control of the computer, and used to encode key information. The corresponding sector states are $|\chi_1\rangle^0$, $|\chi_2\rangle^0$, ..., $|\chi_N\rangle^0$, which are the designed holograms for key elements 1, 2, ..., N, respectively. For a stream of key elements, Bob can successively choose the corresponding phase holograms and modulate them in his SLM controlled by the computer.
4) In Alice's private space, the length of the SMF_{A2} and SMF_{A3} can control the signal photons and the idle photons simultaneously to reach D_{A1} and D_{A2}. Later in the experiment, Alice makes use of the information sent by the D_{A1} and the D_{A2} for coincidence measurement and decoding.

By the Equation (6), the coincidence rate and the difference of the random variable rotation angle θ of the polarization states and the random variable angle χ of the OAM sector states are the relationship between cosine square.

In according to coincidence measurement, Alice and Bob can perform the following QKD; if the random variable rotation angle θ of the polarization states is fixed for one photon at Alice's side (θ can be fixed at $\pi/2$), and some discrete χ with different angles are prepared for the other photon at Bob's side. Finally, Alice utilizes different coincidence counting approaches to retrieve the key code sent by Bob. In practice, the agreement between the encoding and the decoding is presented as follows: In the sending end, Bob randomly

modulates the OAM sector states variable angle χ, when χ is 0 yards '00', when χ is $\pi/4$ yards '01', when χ is $\pi/2$ yards '10'. In the receiving end, Alice provides each pair of the corresponding signal and idle photons the time to arrive for coincidence measurement. If the coincidence counting is '0', then the code is '00'; if the coincidence counting is '0.5', then the code is '01'; If the coincidence counting is '1', then the code is '10'. In according to her own coincidence counting, Alice aims to establish a random stream 00, 01, 10 as a codebook. On the basis of the different coincidence rates, Alice can retrieve the key stream sent by Bob. Thus they can share the same keys.

IV. PERFORMANCE ANALYSIS

A. PURIFICATION RATE ANALYSIS

When the QP transforms the polarization states into the OAM states, the conversion rate of the QP is usually 0.80 ± 0.05. Therefore, there are the deviation 0.20 ± 0.05 polarization entangled states, which are not transformed. In other words, the photons coming out from the QP still exist polarization entangled states, which are not transformed. Fidelity is a physical quantity, which is used for describing the similar degree between the state of original condition and the quantum state during the transmission. Fidelity can be used to give a description of the similar degree between the state of evolution, the initial quantum state and the transmission state over time in the process. Fidelity is defined as $F(\rho_1, \rho_2) = [Tr(\sqrt{\rho_1}\rho_2\sqrt{\rho_1})^{\frac{1}{2}}]^2$, where ρ_1 and ρ_2 denote the state density operator corresponding to two kinds of quantum states respectively. The fidelity value of quantum states is between 0 and 1. If the fidelity value of quantum states is 0, then the transmission state over time in the process is a totally different quantum state in comparison with the initial quantum state. If the fidelity value of the quantum states is 1, then the initial quantum state and the transmission state over time in the process are exactly the same. If $0 < F(\rho_1, \rho_2) < 1$, there are some differences and partial distortion between the initial quantum state and the transmission state over time in the process. Thereby, the hybrid entangled states are produced through the QP, whose optimal fidelity is 0.957 ± 0.002 in ideal conditions, however, in the actual experiments, the fidelity is restricted by the linear entropy 0.012 ± 0.002 of hybrid entangled states [31]. Consequently, some parts of the process of transforming polarization states into OAM states have been incomplete given the characteristic of the QP, as depicted in Figure 6. Through a feedback compensation loop, the polarization entangled states which are not transformed (the above-mentioned more than 20%) are sent to the input of the QP and converted again. Through the transformation of the QP, the polarization entangled states which are not transformed and the hybrid entangled states go into the purification setup again. After the purification setup, the high-purity hybrid entangled states are directly output, and the polarization entangled states that are not transformed access the feedback compensation loop again. The feedback compensation setup is a loop, as long as there are the polarization entangled states which are not transformed, the feedback compensation will always continue. When the times of the feedback compensation is n, the conversion rate of polarization entangled states is depicted by $\alpha_p(n) = 1 - (1 - 80\%)^{n+1}$. When $n = 3$, $\alpha_p(3) = 1 - (1 - 80\%)^{3+1} = 99.84\%$, that is, when the times of the feedback compensation is 3, the conversion rate has reached 99.84%.

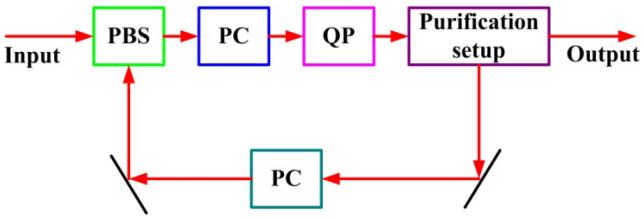

FIGURE 6. Schematic Block Diagram of feedback compensation loop. PBS: polarization beam splitter; PC: polarization controller; QP: q-plate.

The purification setup, which is composed of M-Z interferometer and the BR, no matter what the topological charge of OAM is, can make use of this setup for purification by means of appropriate cascade, thus improve the conversion rate of polarization-OAM, enhancing the anti-interference performance, and increasing the amount of information.

In the informatics, if a source has m kinds of messages, and each message is equal to a probability, the amount of information of this source can be represented as $I = \log_2{}^m$ qubits. In this proposed QKD system, there is the modulation of polarization-OAM multi-degrees of freedom; hence the amount of information of this source can be represented as $I = \log_2{}^m + 1$ qubits. The comparison of the scheme demonstrated in the article and the literatures [20]–[22] and [31] is depicted in Table 1.

B. SECURITY ANALYSIS

In this scenario, the hybrid entangled states are obtained through the purification of specific optical structure and the filtration of SMF in the link. When these high purity hybrid entangled states are applied to the QKD scheme, the states themselves will bring quantum bit error rate, which is very low to this solution. For another, in QKD, for the ATB way, Eve intercepts the uncoded photons, and for the BTA way, Eve intercepts the photons with $l = 0$ mode, which have no key information and not for coincidence measurement, so Eve cannot obtain any key information from all of the two ways. Once more, weak pulse may contain more than one photon; Eve easily intercepted some photons and sent other photons to Bob. Of course, during the coincidence measurement of the scheme, Eve could also keep some photons, and send other photons to Bob. However, according to the characteristics of entangled photon pairs, in the first place, if Eve intercepts some photons from any one road, and the coincidence measurement needs photons from two roads, so Eve can't make the retained photons conform to coincidence measurement.

TABLE 1. Comparison of five schemes.

Scheme	Entanglement type	Cascade purification	Conversion rate	Coincidence rate	Estimated amount of information (bit)
Reference [20]	Polarization	—	—	—	2
Reference [21]	OAM	—	—	$\cos^2 l(\theta_A-\theta_B)$	$\log_2^m$
Reference [22]	SAM-OAM	—	$<80\%$	$\cos^2(2\chi-\theta)$	$\log_2^m+1$
Reference [31]	Polarization-OAM	—	$<80\%$	—	Not given
Proposed Method	Polarization-OAM	Level 3	99.84%	$\cos^2(\chi-\theta)$	$\log_2^m+1$

In the second place, if Eve intercepts some photons from two roads, and the coincidence measurement needs photons from two roads which are detected at the same time and achieve the coincidence counter at the same time, so Eve can't make the retained photons conform to coincidence measurement. In conclusion, Eve cannot generate any key information carried by the photons she retained; this scheme can rise superior to the Man-in-the-middle attack (MITM) attack. The MITM is an ''indirect'' attack in which a computer controlled by an intruder is placed virtually between two communicating computers connected to a network through various techniques. Moreover, Eve can take despite several eavesdropping strategies to obtain key information, such as the IR attack and the MITM attack, but according to the entanglement properties and the principle of coincidence measurement, Eve still can't get the useful key information.

C. HIGH-DIMENSIONAL ENCODING OF MULTI-DEGREE OF FREEDOM

In the light field, the energy in the screw on the harmonic consists of light spectrum of the OAM, and every photon carries the OAM with $l\hbar$. l can take arbitrary integer, so the OAM has an infinite number of eigenstates. In other words, if the OAM characteristic is used to describe information, the OAM states can carry an infinite amount of information. In this solution, high purity polarization-OAM hybrid entangled states are generated through entanglement preparation carrying the OAM light. That is, if the OAM degree of freedom, which has a high-dimensional feature, is used in this solution, then quantum information processing is high dimensional and expandable with these hybrid entangled states.

If the parameters of the QP are selected the topological charges of the OAM are fixed. This article selects $l = 1$, of course, if there are multiple QP with appropriate cascade, higher order value l can be obtained and used to realize the high-dimensional encoding feature.

V. CONCLUSION

The QKD scheme for internet of IoV, which is based on high purity polarization-OAM hybrid entangled states, is proposed in this paper, and it further develops the technical solution of the references [22] and [31]. The purification setup, which consists of M-Z interferometer and the BR, can prepare accurate purity hybrid entangled states, and the cascade feedback can improve the conversion rate of the QP. Furthermore, it can provide efficient and low latency communication and computation. This simple and available QKD scheme can adopt multi-degree of freedom for high-dimensional and secure encoding. Precise purity hybrid entangled states can control distortion of information and ensure insensitive to experimental condition and environmental noise. In this scheme, the MUBs are not employed in the process of this QKD, which makes this program efficient and simple. Moreover, the scheme based on hybrid entangled states can be used for IoT, IoV, cloud computing based big data mining, online optimization for real-time traffic data, and quantum authentication.

APPENDIX

The following abbreviations are used in this manuscript:

QKD	Quantum Key Distribution
OAM	Orbital Angular Momentum
SPDC	Spontaneous Parametric Down-Conversion
QP	q-plate
SMF	Single Mode Fiber
BR	Beam Rotator
PBS	Polarization Beam Splitter
SLM	Spatial Light Modulator
MUBs	Mutually Unbiased Bases
BS	Beam Splitter
LD	Laser Diode
PC	Polarization Controller
DP	Dove Prism
QWP	Quarter Wave Plate
HWP	Half Wave Plate
D	Detector
M	Mirror

ACKNOWLEDGMENT

(Jianjun Guo and Keqiang Wang contributed equally to this work.)

REFERENCES

[1] R. Zhu, X. Zhang, X. Liu, W. Shu, T. Mao, and B. Jalaeian, "ERDT: Energy-efficient reliable decision transmission for intelligent cooperative spectrum sensing in industrial IoT," *IEEE Access*, vol. 3, pp. 2366–2378, 2015.

[2] O. Kaiwartya, A. H. Abdullah, Y. Cao, A. Altameem, M. Prasad, C.-T. Lin, and X. Liu, "Internet of vehicles: Motivation, layered architecture, network model, challenges, and future aspects," *IEEE Access*, vol. 4, pp. 5356–5373, 2016.

[3] F. Yang, S. Wang, J. Li, Z. Liu, and Q. Sun, "An overview of Internet of vehicles," *China Commun.*, vol. 11, no. 10, pp. 1–15, Oct. 2014.

[4] X. Liu, R. Zhu, A. Anjum, J. Wang, H. Zhang, and M. Ma, "Intelligent data fusion algorithm based on hybrid delay-aware adaptive clustering in wireless sensor networks," *Future Gener. Comput. Syst.*, vol. 104, pp. 1–14, Mar. 2020.

[5] M. A. Habib, M. Ahmad, S. Jabbar, S. Khalid, J. Chaudhry, K. Saleem, J. J. P. C. Rodrigues, and M. S. Khalil, "Security and privacy based access control model for Internet of connected vehicles," *Future Gener. Comput. Syst.*, vol. 97, pp. 687–696, Aug. 2019.

[6] H. H. R. Sherazi, R. Iqbal, F. Ahmad, Z. A. Khan, and M. H. Chaudary, "DDoS attack detection: A key enabler for sustainable communication in Internet of vehicles," *Sustain. Comput., Inform. Syst.*, vol. 23, pp. 13–20, Sep. 2019.

[7] Z. Huang, X. Xu, J. Ni, H. Zhu, and C. Wang, "Multimodal representation learning for recommendation in Internet of Things," *IEEE Internet Things J.*, vol. 6, no. 6, pp. 10675–10685, Dec. 2019.

[8] A. Einstein, B. Podolsky, and N. Rosen, "Can quantum-mechanical description of physical reality be considered complete?" *Phys. Rev.*, vol. 47, pp. 777–780, May 1935.

[9] E. Wakakuwa, A. Soeda, and M. Murao, "Complexity of causal order structure in distributed quantum information processing: More rounds of classical communication reduce entanglement cost," *Phys. Rev. Lett.*, vol. 122, no. 19, May 2019, Art. no. 190502.

[10] S. Roy, T. Chanda, T. Das, A. Sen(De), and U. Sen, "Deterministic quantum dense coding networks," *Phys. Lett. A*, vol. 382, no. 26, pp. 1709–1715, Jul. 2018.

[11] S. Ma, Z. Liu, C. Wang, C. Hu, E. Li, W. Gong, Z. Tong, J. Wu, X. Shen, and S. Han, "Ghost imaging LiDAR via sparsity constraints using push-broom scanning," *Opt. Express*, vol. 27, no. 9, p. 13219, Apr. 2019.

[12] J. Guo, Y. Liang, X. G. Huang, B. Guo, and J. Li, "Pure dielectric waveguides enable compact, ultrabroadband wave plates," *IEEE Photon. J.*, vol. 8, no. 5, pp. 1–9, Oct. 2016.

[13] M. Ureña, I. Gasulla, F. J. Fraile, and J. Capmany, "Modeling optical fiber space division multiplexed quantum key distribution systems," *Opt. Express*, vol. 27, no. 5, pp. 7047–7063, 2019.

[14] X. Liu, R. Zhu, B. Jalaian, and Y. Sun, "Dynamic spectrum access algorithm based on game theory in cognitive radio networks," *Mobile Netw. Appl.*, vol. 20, no. 6, pp. 817–827, Dec. 2015.

[15] K. Cai, R. Yang, L. Li, S. Ou, Y. Chen, and J. Dou, "A semi-automatic coronary artery segmentation framework using mechanical simulation," *J. Med. Syst.*, vol. 39, no. 10, p. 129, Oct. 2015.

[16] A. K. Ekert, "Quantum cryptography based on Bell's theorem," *Phys. Rev. Lett.*, vol. 67, no. 6, pp. 661–663, Aug. 1991.

[17] J. Guo and L. Lin, "An on-chip chiral converter and polarization rotator," *Optik*, vol. 202, Feb. 2020, Art. no. 163740.

[18] A. Poppe, A. Fedrizzi, R. Ursin, H. R. Böhm, T. Lorünser, O. Maurhardt, M. Peev, M. Suda, C. Kurtsiefer, H. Weinfurter, T. Jennewein, and A. Zeilinger, "Practical quantum key distribution with polarization entangled photons," *Opt. Express*, vol. 12, no. 16, pp. 3865–3871, 2014.

[19] I. Marcikic, A. Lamas-Linares, and C. Kurtsiefer, "Free-space quantum key distribution with entangled photons," *Appl. Phys. Lett.*, vol. 89, no. 10, Sep. 2006, Art. no. 101122.

[20] F. Kaiser, A. Issautier, L. A. Ngah, O. Alibart, A. Martin, and S. Tanzilli, "A versatile source of polarization entangled photons for quantum network applications," *Laser Phys. Lett.*, vol. 10, no. 4, Apr. 2013, Art. no. 045202.

[21] S.-M. Zhao, L.-Y. Gong, Y.-Q. Li, H. Yang, Y.-B. Sheng, and W.-W. Cheng, "A large-alphabet quantum key distribution protocol using orbital angular momentum entanglement," *Chin. Phys. Lett.*, vol. 30, no. 6, Jun. 2013, Art. no. 060305.

[22] C. Zhang, B. Guo, G. Cheng, J. Guo, and R. Fan, "Spin-orbit hybrid entanglement quantum key distribution scheme," *Sci. China Phys., Mech. Astron.*, vol. 57, no. 11, pp. 2043–2048, Nov. 2014.

[23] G. Vallone, V. D'Ambrosio, A. Sponselli, S. Slussarenko, L. Marrucci, F. Sciarrino, and P. Villoresi, "Free-space quantum key distribution by rotation-invariant twisted photons," *Phys. Rev. Lett.*, vol. 113, no. 6, Aug. 2014, Art. no. 060503.

[24] Z. Y. Ou and L. Mandel, "Violation of Bell's inequality and classical probability in a two-photon correlation experiment," *Phys. Rev. Lett.*, vol. 61, no. 1, pp. 50–53, Jul. 1988.

[25] L. Allen, M. W. Beijersbergen, R. J. C. Spreeuw, and J. P. Woerdman, "Orbital angular momentum of light and the transformation of Laguerre–Gaussian laser modes," *Phys. Rev. A, Gen. Phys.*, vol. 45, no. 11, pp. 8185–8189, Jun. 1992.

[26] B. Wu, T. T. Cheng, T. L. Yip, and Y. Wang, "Fuzzy logic based dynamic decision-making system for intelligent navigation strategy within inland traffic separation schemes," *Ocean Eng.*, vol. 197, Feb. 2020, Art. no. 106909.

[27] M. Malik, M. Mirhosseini, M. P. J. Lavery, J. Leach, M. J. Padgett, and R. W. Boyd, "Direct measurement of a 27-dimensional orbital-angular-momentum state vector," *Nature Commun.*, vol. 5, no. 1, p. 3115, May 2014.

[28] A. Mair, A. Vaziri, G. Weihs, and A. Zeilinger, "Entanglement of the orbital angular momentum states of photons," *Nature*, vol. 412, no. 6844, pp. 313–316, Jul. 2001.

[29] K. Cai, R. Yang, H. Chen, L. Li, J. Zhou, S. Ou, and F. Liu, "A framework combining window width-level adjustment and Gaussian filter-based multi-resolution for automatic whole heart segmentation," *Neurocomputing*, vol. 220, pp. 138–150, Jan. 2017.

[30] Z. Huang, X. Xu, H. Zhu, and M. Zhou, "An efficient group recommendation model with multiattention-based neural networks," *IEEE Trans. Neural Netw. Learn. Syst.*, early access, Jan. 15, 2020, doi: 10.1109/TNNLS.2019.2955567.

[31] E. Nagali and F. Sciarrino, "Generation of hybrid polarization-orbital angular momentum entangled states," *Opt. Express*, vol. 18, no. 17, pp. 18243–18248, 2010.

[32] Z. Chen, H. Cai, Y. Zhang, C. Wu, M. Mu, Z. Li, and M. A. Sotelo, "A novel sparse representation model for pedestrian abnormal trajectory understanding," *Expert Syst. Appl.*, vol. 138, Dec. 2019, Art. no. 112753.

[33] M. Christandl and R. Renner, "Reliable quantum state tomography," *Phys. Rev. Lett.*, vol. 109, no. 12, Sep. 2012, Art. no. 120403.

[34] J. Leach, M. J. Padgett, S. M. Barnett, S. Franke-Arnold, and J. Courtial, "Measuring the orbital angular momentum of a single photon," *Phys. Rev. Lett.*, vol. 88, no. 25, Jun. 2002, Art. no. 257901.

[35] C. Gao, X. Qi, Y. Liu, J. Xin, and L. Wang, "Sorting and detecting orbital angular momentum states by using a Dove prism embedded Mach–Zehnder interferometer and amplitude gratings," *Opt. Commun.*, vol. 284, no. 1, pp. 48–51, 2011.

[36] L. Chen and W. She, "Teleportation of a controllable orbital angular momentum generator," *Phys. Rev. A, Gen. Phys.*, vol. 80, no. 6, Dec. 2009, Art. no. 063831.

[37] J. Guo, B. Guo, R. Fan, W. Zhang, Y. Wang, L. Zhang, and P. Zhang, "Measuring topological charges of Laguerre–Gaussian vortex beams using two improved Mach–Zehnder interferometers," *Opt. Eng.*, vol. 55, no. 3, Mar. 2016, Art. no. 035104.

[38] P. G. Kwiat, E. Waks, A. G. White, I. Appelbaum, and P. H. Eberhard, "Ultrabright source of polarization-entangled photons," *Phys. Rev. A, Gen. Phys.*, vol. 60, no. 2, pp. R773–R776, Aug. 1999.

JIANJUN GUO received the B.E. degree in optical engineering from South China Normal University, Guangzhou, China, in 2012, the M.S. degree in measurement and control technology and instrumentation from the Hebei University of Science and Technology, Shijiazhuang, China, in 2006, and the Ph.D. degree in optics from South China Normal University, in 2016. He is currently an Associate Professor with the College of Automation, Zhongkai University of Agriculture and Engineering, Guangzhou. His current main research interests include photo-communication, image recognition, and information safety.

KEQIANG WANG received the M.E. degree in theoretical physics from Jiangxi Normal University, Nanchang, China, in 1993. He is currently a Professor with the College of Automation, Zhongkai University of Agriculture and Engineering, Guangzhou. His current main research interests include intelligent robot, agricultural informatization, deep learning, and agricultural automation.

FENGMEI YU received the B.E. degree in physics education from Shenyang Normal University, Shenyang, China, in 2000, the M.E. degree in condensed matter physics from Guangzhou University, Guangzhou, China, in 2003, and Ph.D. degree in condensed matter physics from Sun Yat-sen University, Guangzhou, China, in 2014. She is currently an Associate Professor with the Zhongkai University of Agriculture and Engineering. Her research interests include transport and magnetic properties of films, and nonlinear optical properties of low dimensional semiconductor materials, and electrical and electronic technology.

KEN CAI received the Ph.D. degree in biomedical engineering from the South China University of Technology, China, in 2011. He is currently a Professor with the College of Automation, Zhongkai University of Agriculture and Engineering, China. His current main research interests include medical data analytic, deep learning, pattern recognition, and decision making and biomedical instrument.